

## Enhancement of Photoelectric Efficiency in a Dye-sensitized Solar Cell Using Hollow TiO<sub>2</sub> Nanoparticles as an Overlayer

Kyoung-No Lee, Woo-Byoung Kim,<sup>†</sup> Caroline Sunyong Lee, and Jai-Sung Lee\*

Department of Metallurgy and Materials Science, Hanyang University, Ansan 426-791, Korea. \*E-mail: jslee@hanyang.ac.kr

<sup>†</sup> Department of Energy Engineering, Dankook University, Chungnam 330-714, Korea

Received March 26, 2013, Accepted April 20, 2013

TiO<sub>2</sub> hollow nanoparticles (HNPs) and their light scattering effect which influences on the photoelectric conversion efficiency of a dye-sensitized solar cell (DSSC) were investigated. When only HNPs were employed in DSSC as the anode layer material, the conversion efficiency (e.g., 0.96%) was the lowest, possibly due to scattering loss of incident light. However, DSSC fabricated by using HNPs as a scattering overlayer on the TiO<sub>2</sub> nanoparticles (P-25), showed higher conversion efficiency (4.02%) than that without using HNPs (3.36%).

**Key Words :** DSSC, TiO<sub>2</sub> hollow nanoparticles, Scattering layer, CVC

### Introduction

Dye-sensitized solar cells (DSSC) have attracted much attention as the next generation solar cell because of its low production costs and high energy conversion efficiency.<sup>1,2</sup> Therefore, many research groups have focused on how to improve the photo-current of DSSC and/or how to optimize electrolyte components and structures.<sup>3-8</sup> Such improvements of the light harvesting efficiency of the DSSC can be achieved by enlarging the specific surface area of the TiO<sub>2</sub> electrodes and/or by inserting light scattering structures. Particularly, some light-scattering structures such as large-size of TiO<sub>2</sub> spheres and/or rods showed that the light trapping within the DSSC was available.<sup>9-12</sup> However, by inserting the large-sized scattering layer, the total specific surface area of electrode is decreased.<sup>9</sup> In other words, the low dye-adsorption due to the large size of materials still remains as a problem to overcome in order to enhance the electricity conversion efficiency.

In this respect, a recent report by H. J. Koo and colleagues, regarding a DSSC electrode consisting of nano-embossed hollow spherical TiO<sub>2</sub> particles, gives a notable message that conversion efficiency is possibly enhanced (21% increase) by changing particle shape.<sup>13</sup> Moreover, the enhancement is attributed to the light scattering of nano-embossed hollow spheres occurred in the longer wavelength region and the higher dye adsorption compared to the large-sized TiO<sub>2</sub>. However, it should be noted that the nano-embossed hollow structure still has lower dye adsorption than nanocrystalline TiO<sub>2</sub> does. Especially, the effect of TiO<sub>2</sub> HNPs in DSSC has not been studied. For this reason, TiO<sub>2</sub> hollow nanoparticles less than 30 nm in particle size, were applied to increase the dye adsorption for the application of DSSC.<sup>14-17</sup>

Thus, the effect of the hollow nanostructure of TiO<sub>2</sub> particles on the performance of DSSC was evaluated. In order to achieve the goal, we synthesized TiO<sub>2</sub> hollow nanoparticles (HNPs) by the gas phase synthesis route and ap-

plied the HNP samples to the anode of DSSC. In addition, three different anode structures of HNPs, commercial TiO<sub>2</sub> particles (P-25), and the mixture of HNPs and P-25, were prepared and tested to understand the effect of hollow nanostructure on the conversion efficiency.

### Experimental

Titanium oxide acetylacetonate, TiO(C<sub>5</sub>H<sub>7</sub>O<sub>2</sub>)<sub>2</sub> (Sigma-Aldrich), was used as a precursor for the synthesis of TiO<sub>2</sub> hollow nanoparticles (HNPs). Detailed process condition including gas flow rate to prepare TiO<sub>2</sub> HNPs was described in the previous study.<sup>17</sup> As-received TiO<sub>2</sub> HNPs and commercial TiO<sub>2</sub> nanoparticles, (Degussa P-25) were made into paste using ethyl cellulose and  $\alpha$ -terpineol. Then, the paste was screen-printed on the transparent conducting oxide (TCO) glass substrate (F-doped, Nippon Sheet Glass Co.) with a thickness of 16  $\mu$ m and subsequently sintered at 500 °C in air atmosphere. Diluted N-719 dye ( $3 \times 10^{-4}$  mole, Solaronix Co.,) was chemisorbed on the surface of the thin TiO<sub>2</sub> film.

The crystal phase and crystallite size of the TiO<sub>2</sub> samples were analyzed by X-ray Diffraction (XRD, Rigaku Denki, D/MAX-2500 PC). And specific surface area was measured by nitrogen adsorption (Autosorb-1) using BET method. Morphologies of the samples were observed using transmission electron microscopy (TEM, Model No. JEOL Co.,). Finally, the incident photo-to-current conversion efficiency was measured by solar simulator (SERIC Co.,) under A.M. 1.5 (96.102 mW/cm<sup>2</sup>).

### Results and Discussion

Figure 1(a) shows the XRD patterns of TiO<sub>2</sub> HNP and P-25 nanoparticle samples. It is clearly found that the two samples commonly consist of an anatase-dominant anatase/rutile mixed phase. The relative ratio of anatase and rutile

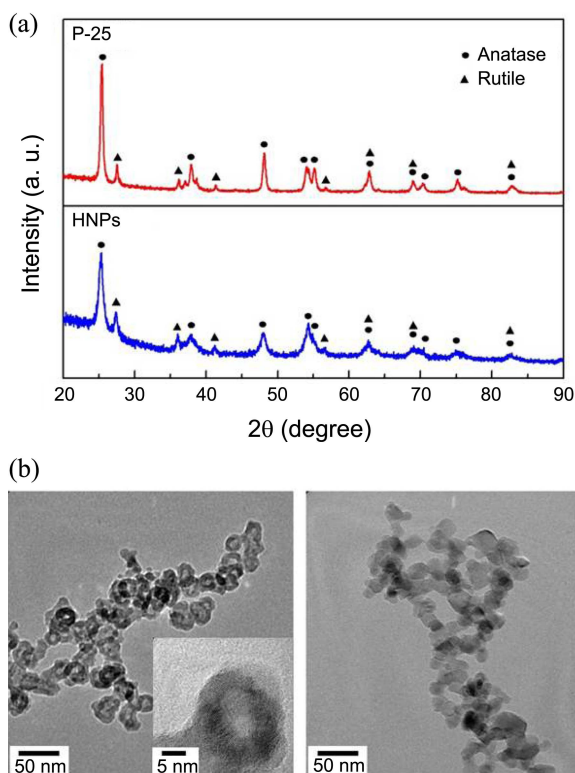


**Figure 1.** X-ray diffraction patterns (a) and TEM micrographs (b) of TiO<sub>2</sub> hollow nanoparticles and P-25 nanoparticles.

phases was estimated to be 77% in vol. (anatase) and 23% in vol. (rutile) using HNPs, 86% (anatase) in vol. and 14% (rutile) in volume using P-25 only. The crystallite size of HNPs and P-25 calculated according to the Scherrer equation, was found to be 17 nm and 22 nm, respectively.

Figure 1(b) shows TEM micrographs of the HNPs and P-25 samples. First the P-25, which is a sample consisted of dense TiO<sub>2</sub> nanoparticle, has a uniform size distribution in the range of 20–30 nm, which is in good agreement with the crystallite size as shown in XRD pattern in Figure 1(a). On the other hand, the sample consisting of HNP showed a typical hollow nanostructure with a shell thickness of 3–5 nm and a narrow particle size distribution ranging from 20 to 25 nm. As shown in the previous study,<sup>17</sup> it is reconfirmed that the HNPs have shells and the pores inside. Also, the shell of each HNP with no open pores was found to consist of several grains with different crystallographic orientations. Thus, the calculated crystallite size of the HNPs (17 nm), which is smaller than the observed size by TEM (20–25 nm), might be due to the nano grains consisting of the shell structure of the HNPs.

The photo-to-current conversion efficiency of the DSSC substantially depends on the dye adsorption rate on the surface of the TiO<sub>2</sub> film. Also, TiO<sub>2</sub> nanoparticles used as the scattering layer, necessarily require a unique particle shape that can provide larger specific surface area. However, the surface area was measured to be 60 m<sup>2</sup>/g for the HNPs and 62 m<sup>2</sup>/g for the P-25, respectively. Table 1 shows that there is nearly no difference in surface area between both

**Table 1.** The results of phase analysis and particle characteristics of TiO<sub>2</sub> hollow nanoparticles and P-25 nanoparticles using XRD and BET measurement

	XRD		BET	
	Particle sizes (nm)	Phase	Particle sizes (nm)	Specific surface area (m <sup>2</sup> /g)
HNPs	17	Anatase (77%) Rutile (23%)	26	60
P-25	22	Anatase (86%) Rutile (14%)	25	62

nanoparticle samples within an error range. As described above, the apparent size of both nanoparticles estimated from TEM observation looks nearly the same in the range of 20 nm and also the surface of HNPs have closed structure without open pores. Accordingly, it is believed that increase in surface area has no effect on the dye adsorption rate between both nanoparticle samples.

Figure 2 shows the optical transmittance of the HNP and P-25 samples in the range of 300–800 nm in wavelength. The transmittance of the P-25 nanoparticles is over 85% in the visible light region, while the HNPs is less than 20%. It is thought that this low transmittance of HNP sample results from the light scattering of the hollow nanostructure. It has been known that different refractive index materials induce the light scattering.<sup>18</sup> From this point of view, the light scattering at the boundary between the shell and inner pore might be more vigorous for HNP sample than that for dense nanoparticles. Moreover, the multi-refraction inside of the hollow structure and/or hollow structure layer can additionally increase the number of light scattering and the path length of incident light, resulting in enhanced scattering intensity.<sup>19</sup> It is thus expected that the photo-current density can increase due to the scattering effects without degradation of the amount of adsorbed dye molecule when the HNPs are employed in the DSSC as the material for scattering layer.

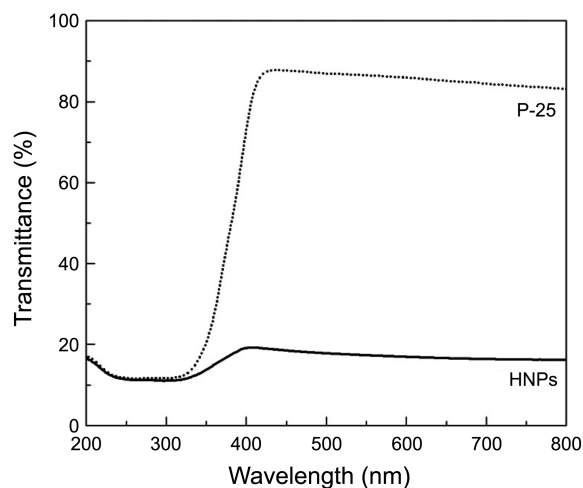


**Figure 2.** Optical transmittance spectra of TiO<sub>2</sub> hollow nanoparticles and P-25 nanoparticles.

Figure 3(a) represents the photo-current vs. voltage curves of three different DSSC anode structures prepared by HNPs, P-25 and mixed nanoparticles. Table 2 further lists the results for the related photo-voltaic parameters of three kinds of solar cells. It is found that the photo-current density of the anode TiO<sub>2</sub> film fabricated only by the HNPs is lower than that using nanocrystalline TiO<sub>2</sub> film (P-25), resulting in lower conversion efficiency (*i.e.*, 0.96% for the only HNPs and 3.36% for the P-25). The Fresnel transmission coefficient for two media can be expressed as follows,

$$T_f = \frac{4n_1n_2}{(n_1+n_2)^2} \quad (1)$$

where,  $n_1$  and  $n_2$  are refractive index of values of media 1 and 2, respectively. The nanocrystalline TiO<sub>2</sub> particles (P-25) have a refractive index  $n_{\text{TiO}_2} = 2.5$ , while the refractive index of HNP was estimated approximately to be  $n_{\text{HNPs}} = 1.6$  since each HNP consists of a closed pore with diameter of 15 nm in size and 5 nm-thick shells.<sup>18</sup> The Fresnel transmission coefficient of P-25 with the acetonitrile solvent, *i.e.*  $n_{\text{acetonitrile}} = 1.34$ , can be calculated to be about 0.91, but the HNPs to be about 0.68. It means that the penetration of incident light to dye can be interrupted by the HNPs structure. Thus, the lower photo-current density is likely to result from the low transmittance of the HNPs ( $\leq 20\%$ ) layer by light scattering and/or multi-refraction. On the contrary, when HNPs (4  $\mu\text{m}$  thickness) layer is employed into a scattering overlayer on the nanocrystalline TiO<sub>2</sub> layer (12  $\mu\text{m}$  thickness), the conversion efficiency of the DSSC is

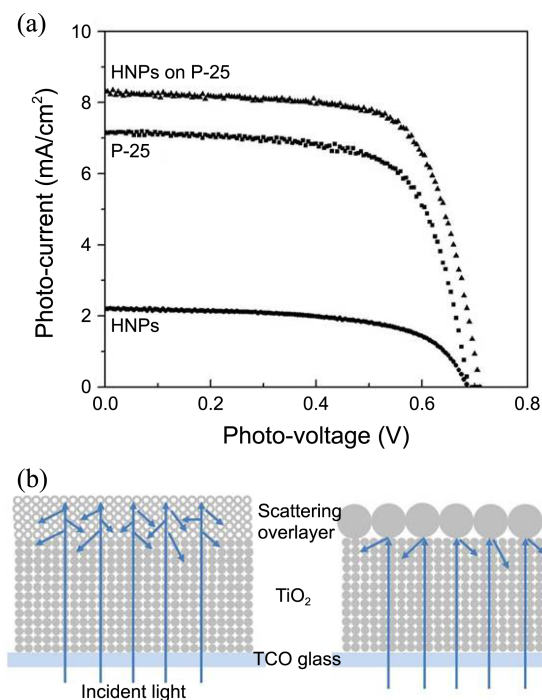


**Figure 3.** Photocurrent-Voltage curves of dye-sensitized solar cells fabricated using three different anode structures: a) TiO<sub>2</sub> hollow nanoparticles, b) P-25 and c) TiO<sub>2</sub> hollow nanoparticles on P-25 (a) and schematic diagrams of the dye-sensitized solar cell consisted of the HNPs and large-sized dense particles overlayers (b).

**Table 2.** Comparison of I-V characteristics of dye-sensitized solar cells formed by three different anode structures: TiO<sub>2</sub> hollow nanoparticles, P-25 nanoparticles and TiO<sub>2</sub> hollow nanoparticles on P-25

	$V_{oc}$ (V)	$I_{sc}$ (mA)	$J_{sc}$ (mA/cm <sup>2</sup> )	$FF$	(%)
HNPs	0.69	0.53	2.12	0.66	0.96
P-25	0.69	1.76	7.42	0.69	3.36
HNPs on P-25	0.71	2.05	8.00	0.69	4.02

improved from 3.36% (nanocrystalline TiO<sub>2</sub> layer) to 4.02% due to improved photo-current density, by 20% increment. Such an improvement of the higher photo-current density of the HNPs on P-25 TiO<sub>2</sub> film should be attributed to the TiO<sub>2</sub> hollow structure which is beneficial for light scattering because of multi-refraction within the hollow structure. Due to low refractive index of the HNPs, some of the incident light will be scattered in the HNPs layer and the other will pass through until they meet other HNPs layer or an electrolyte. Therefore, the conversion efficiency of HNPs is much higher than that of P-25, and it also expected that the conversion efficiency of the HNPs is higher than that of scattering layer with large size of TiO<sub>2</sub> particles due to multi-refractive effect of the HNPs. Figure 3(b) shows the schematic diagram of the incident light scattering effects using two different structures formed by the HNPs, and large-sized and dense particles overlayers. The size of HNPs in this study, is close to that of the P-25 nanoparticles. It means that the specific surface area was decreased despite of using scattering layer compared to large-sized using dense particles. Hence, even if the scattering effect of the HNPs is similar to pre-reported scattering layers,<sup>19</sup> the photo current should be higher than that of large-sized and dense particles.

Figure 4 displays the incident photo to current conversion efficiency (IPCE) of DSSC using HNPs and P-25, and HNPs

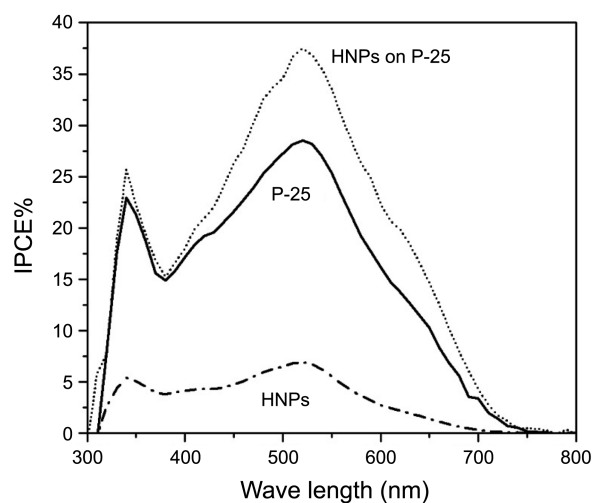


**Figure 4.** Incident photo to current conversion efficiency (IPCE) spectra of dye-sensitized solar cells formed by three different anode structures: a) TiO<sub>2</sub> hollow nanoparticles, b) P-25 and c) TiO<sub>2</sub> hollow nanoparticles on top of P-25.

on P-25 as a function of wavelength. The IPCE spectra showed the maximum value at 530 nm using N-719 dye.<sup>20</sup> It was reported that the absolute intensity of the IPCE in the short wavelength region (*i.e.*, 400 to 570 nm) is attributed to dye absorption rate and a higher value of the IPCE in the long wavelength is attributed to scattering effects because more light is transmitted through the TiO<sub>2</sub> electrode and scattered in this region.<sup>13</sup> The absolute IPCE of the HNPs on P-25 sample is higher than that of the P-25, which is in good agreement with the higher  $J_{sc}$  as observed in the I-V measurement result. Generally, it is believed that the hollow structure as the scattering overlayer, only affects the long wavelength region because of decrease in specific surface area.<sup>21</sup> However, in the case that the HNPs are used as the scattering overlayer in combination with P-25, the intensity of IPCE increased not only in the long wavelength region but also in the short wavelength due to the multi-scattering of the nano-sized hollow particles. On the other hand, the IPCE of the scattering layer consisting of only the HNPs showed the lowest intensity, which might be due to scattering loss of the incident light instead of decreasing dye absorption.

### Conclusion

In conclusion, the authors investigated light scattering effect of TiO<sub>2</sub> hollow nanoparticles (HNPs) on the electricity conversion efficiency of the dye-sensitized solar cells (DSSC). The HNPs was synthesized by CVC process, and their mean particle size, specific surface area and crystalline phase were almost identical to those for P-25. When the HNPs were only employed in DSSC as the anode layer, low conversion efficiency (*e.g.*, 0.96%) was obtained due to its scattering loss of incident light. On the other hand, when the HNPs were introduced as a scattering overlayer on top of P-25, the conversion efficiency of DSSC increased by 20% because of its multi-scattering effect of hollow nanostructure and larger

specific surface area. Therefore HNP as an overlayer in DSSC, was found to be beneficial.

### References

1. O'regan, B.; Gratzel, M. *Nature* **1991**, 353, 737.
2. Dai, S.; Weng, J.; Sui, Y.; Shi, C.; Huang, Y.; Chen, S.; Pan, X.; Fang, X.; Hu, L.; Kong, F. *Sol. Energy Mater. Sol. Cells* **2004**, 84, 125.
3. Yu, K.; Chen, J. *Nanoscale Res. Lett.* **2009**, 4, 1.
4. Liu, B.; Aydil, E. S. *J. Am. Chem. Soc.* **2009**, 131, 3985.
5. Yoon, J. H.; Jang, S. R.; Vittal, R.; Lee, J.; Kim, K. J. *J. Photochem. Photobiol. A* **2006**, 180, 184.
6. Adachi, M.; Murata, Y.; Takao, J.; Jiu, J.; Sakamoto, M.; Wang, F. *J. Am. Chem. Soc.* **2004**, 126, 14943.
7. Zhu, K.; Neale, N. R.; Miedaner, A.; Frank, A. J. *Nano Lett.* **2007**, 7, 69.
8. Qian, J.; Liu, P.; Xiao, Y.; Jiang, Y.; Cao, Y.; Ai, X.; Yang, H. *Adv. Mater.* **2009**, 21, 3663.
9. Kang, S. H.; Kim, J. Y.; Kim, H. S.; Koh, H. D.; Lee, J. S.; Sung, Y. E. *J. Photochem. Photobiol. A* **2008**, 200, 294.
10. Jiu, J.; Isoda, S.; Wang, F.; Adachi, M. *J. Phys. Chem. B* **2006**, 110, 2087.
11. Zhang, Y.; Li, G.; Wu, Y.; Luo, Y.; Zhang, L. *J. Phys. Chem. B* **2005**, 109, 5478.
12. Yu, I. G.; Kim, Y. J.; Kim, H. J.; Lee, C.; Lee, W. I. *J. Mater. Chem.* **2010**, 21, 532.
13. Koo, H. J.; Kim, Y. J.; Lee, Y. H.; Lee, W. I.; Kim, K.; Park, N. G. *Adv. Mater.* **2008**, 20, 195.
14. Lee, C. W.; Lee, K. W.; Lee, J. S. *Mater. Lett.* **2008**, 62, 2664.
15. Lee, J. S.; Im, S. S.; Lee, C. W.; Yu, J. H.; Choa, Y. H.; Oh, S. T. *J. Nanopart. Res.* **2004**, 6, 627.
16. Lee, J. S.; Lee, C. W.; Lee, K. N. *ICC3: Materials Science and Engineering* **2011**, 18, 062003.
17. Lee, S. C.; Lee, C. W.; Lee, J. S. *Mater. Lett.* **2008**, 62, 564.
18. Ferber, J.; Luther, J. *Sol. Ener. Mater. Sol. Cells* **1998**, 54, 265.
19. Lee, J. K.; Jeong, B. H.; Jang, S. I.; Yeo, Y. S.; Park, S. H.; Kim, J. U.; Kim, Y. G.; Jang, Y. W.; Kim, M. R. *J. Mater. Sci: Mater. Electron.* **2009**, 20, 446.
20. Grätzel, M. *Inorg. Chem.* **2005**, 44, 6841.
21. Yu, H.; Yu, J.; Cheng, B.; Liu, S. *Nanotechnology* **2007**, 18, 065604.